17-Allylamino-Demethoxygeldanamycin Ameliorate Microthrombosis Via HSP90/RIP3/NLRP3 Pathway After Subarachnoid Hemorrhage in Rats

Yuchun Zuo, Tibiao He, Peiqiang Liao, Kai Zhuang, Xiaoxin Yan, and Fei Liu

Abstract *Background*: Subarachnoid hemorrhage (SAH) is a severe and emergent cerebrovascular disease, the prognosis of which usually very poor. Microthrombi formation highlighted with inflammation occurs early after SAH. As the main cause of DCI, microthrombosis associated with the prognosis of SAH. The aim of this study was to show HSP90 inhibitor 17-AAG effect on microthrombosis after SAH in rats.

Methods: Ninety-five SD rats were used for the experiment. For time course study, the rats were randomly divided into five groups: sham group and SAH group with different time point (1d, 2d, 3d, 5d). Endovascular perforation method was conducted for SAH model. Neurological score, SAH grade, and mortality were measured after SAH. The samples of the left hemisphere brain were collected. The expression of HSP90 was detected by Western blot. The microthrombosis after SAH in rats' brain was detected by immunohistochemistry. For mechanism study, rats were randomly divided into three groups: sham, SAH + vehicle, and SAH +17-AAG (n = 6/group). 17-AAG was given by intraperitoneal injection (80 mg/kg) 1 h after SAH. Neurological function were measured at 24 h after SAH. The expression of RIP3, NLRP3, ASC, and IL-1β was measured by Western blot. Microthrombosis was detected by immunohistochemistry.

Results: Our results showed that the HSP90 protein level increased and peaked at 2 days after SAH. Microthrombosis caused by SAH was increased in 1 day and peaked at 2 days after SAH. Administration HSP90 specific inhibitor 17-AAG reduced expression of RIP3, NLRP3, ASC, and IL-1β, reduced microthrombosis after SAH, and improved neurobehavior when compared to vehicle group.

Conclusions: 17-AAG can ameliorate microthrombosis via HSP90/RIP3/NLRP3 pathway and improve neurobehavior after SAH.

Keywords SAH · 17-AAG · Microthrombosis · HSP90

Introduction

Subarachnoid hemorrhage (SAH) is a severe and emergent cerebrovascular disease with high morbidity and mortality and always leads to poor outcome. SAH mainly affects middle-aged patients and counts a highest fatality in all stroke subtypes, which brings about a huge burden on economy and society [1]. Inflammation has been extensively studied in early brain injury (EBI) after SAH, which is considered to be the main cause of mortality and lead to poor outcome [2, 3]. NLRP3 inflammasome, as a part of pro-inflammation, has been well established to take part in the pathophysiology of EBI after SAH [4–6].The inflammatory response and its effect on the occurrence of microthrombosis are frequently discussed as potential protagonists.

Microthrombosis, usually found to be dissociation between cerebral vasospasm (CVS) and delayed cerebral ischemia (DCI), regarded as the major cause of neurologic deterioration and consequent poor outcome [7]. Microthrombi were firstly described in patients who were thought to have died of DCI. The autopsy study showed significantly high amounts of microthrombi were found in ischemic regions [8]. Recently, the occurrence of microthrombi was verified after SAH in animal models [9–11]. Furthermore, endothelial cell apoptosis and coagulation induced by inflammation have been well established [7, 12],which were considered the main cause of microthrombosis [10].

17-Allylamino-demethoxygeldanamycin (17-AAG), a specific inhibitor of HSP90, has been proved to show its effect on preventing cell death especially necroptosis [11, 13, 14]. Moreover, necroptosis plays a potential role in

Y. Zuo · T. He · P. Liao · K. Zhuang · F. Liu (✉)
Department of Neurosurgery, The Third Xiangya Hospital, Central South University, Changsha, China

X. Yan
Department of Anatomy, The XiangYa Medical School, Central South University, Changsha, China

R. D. Martin et al. (eds.), *Subarachnoid Hemorrhage*, Acta Neurochirurgica Supplement 127,
https://doi.org/10.1007/978-3-030-04615-6_12,

inflammation [15]. Furthermore, HSP90 inhibition shows its protection effect by attenuating inflammation response [16] and maintaining blood-brain barrier after ischemia stroke [17]. RIP3 has been described as a key protein in NLRP3 inflammasome previously [4, 18]. More recently, HSP90 has been proven to be an upstream regulator of RIP3 in necroptosis [19, 20].More recently, the HSP90 inhibitor can reduce cell death induced by oxygen-glucose deprivation model [19]. Therefore, we hypothesize that 17-AAG reduces microthrombosis via HSP90/RIP3/NLRP3 pathway after SAH.

Methods and Materials

Animals and SAH Model

Adult male Sprague-Dawley rats (250–280 g) were purchased from the Animal Center of Central South University (Changsha, China). Rats were housed in a room with constant temperature (25 °C), humidity control and with a 12/12 h light/dark cycle. Standard animal chow and water were freely available. All the experimental procedures were approved by the Institutional Animal Care and Use Committee of Central South University.

SAH model was conducted by modified endovascular perforation method as previously described. Briefly, rats were anesthetized with chloral hydrate (400 mg/kg, intraperitoneally). The left common carotid artery and external and internal carotid arteries were exposed, and a 4–0 monofilament nylon suture was inserted into the left internal carotid artery through the external carotid artery stump until feeling resistance and then advanced 3 mm to perforate the bifurcation of the anterior and middle cerebral artery. Sham rats underwent identical procedures except the perforation.

Experiment Design

Experiment 1: For the time course experiment, 70 animals were divided randomly into 5 groups (n = 12/group): sham and SAH (1, 2, 3, 5 days (d)) groups. The neurological function was measured by modified Gracia score, and beam balance test was measured. Rats in the sham group underwent a procedure similar to that of the SAH group except perforation; rats in the SAH group underwent perforation and then euthanized in different time point after SAH. At the same time, SAH grade was measured. Then every group was divided into two groups used for Western blot and immunohistochemistry, respectively (n = 6/group).

Experiment 2: For 17-AAG treatment, 36 rats were divided randomly into three groups: sham (n = 6), SAH + vehicle (n = 12), and SAH + 17-AAG (n = 12). Modified Gracia score and beam balance test were measured. Then every group was divided into two groups used for Western blot and immunohistochemistry, respectively. Brain samples were collected after perfusion by 4% PFA for immunostaining.

Measurement of SAH Grade

As a parameter to evaluate the severity of SAH, SAH grade was obtained according to a grading system that was described previously. Briefly, the system was based on the amount of subarachnoid blood clots distributed in the six segments of basal cistern: grade 1, no subarachnoid blood (score = 0); grade 2, minimal subarachnoid clots (score = 1); grade 3, moderate subarachnoid clots with recognizable arteries (score = 2); and grade 4, blood clots covering all arteries (score = 3). A total score ranging from 0 to 18 was obtained by adding the scores from all six segments. The grading of SAH was performed by a partner who was blinded to the experiment. Rats with the SAH grade lower than 9 were excluded from this study.

Assessment of Neurological Function

The neurological status of all rats was evaluated at 24 h after SAH induction using the previously described modified Garcia scoring system and beam balance test [21].

The assessment of neurological score was performed by a partner who was blind to the experiment.

Western Blot Analysis

Western blot was performed as previously described [22]. Briefly, tissues were extracted by RIPA buffer. The protein concentrations were detected by using a bicinchoninic acid (BCA) assay (Beyotime, Shanghai, China). The protein samples were separated by 10% SDS-polyacrylamide gel electrophoresis (PAGE) and transferred to polyvinylidene fluoride membranes (Millipore, USA). After blocked, the membranes were incubated overnight at 4 °C with the following primary antibodies: anti-HSP90 (1:1000, Proteintech), anti-RIP3 (1:1000, Abcam, USA), anti-NLRP3 (1:500, Abcam, USA), anti-ASC (1:300, Santa Cruz, USA), anti-IL-1β (1:1000, Proteintech), and anti-GAPDH (1:1000,

Proteintech). After incubation with a secondary antibody, the immunocomplexes were visualized by enhanced chemiluminescence (SuperSignal Pierce Biotechnology).

Immunohistochemistry

Immunohistochemistry was performed as previously described [23]. Thirty micrometer coronal brain sections were cut as previously described in a cryostat (Leica CM3050S, Buffalo Grove, IL). Sections from each animal were divided into several subsets for immunohistochemistry. Microthrombi were visualized by immunohistochemistry with fibrinogen staining. After antigen retrieval, the slides were incubated in anti-fibrinogen antibody (1:500) (LifeSpan, Seattle, WA, USA) for 2 h and then incubated by biotinylated secondary antibody (1:400, Abcam, Cambridge, UK) for 1 h and ABC reagents (1:400; Vector Laboratories, Burlingame, CA, USA) for 1 h, with the immunoreactivity visualized in 0.003% H_2O_2 and 0.05% 3, 3′-diaminobenzidine(DAB), and counterstaining was performed with hematoxylin.

Immunofluorescence

Double immunofluorescence staining was performed as previously described [24]. The primary antibodies were biotinylated lectin (1:500, B-1175, Vector), followed by incubation with appropriate fluorescence-conjugated secondary antibody AMCA streptavidin (1:200, SA-5008, Vector). TUNEL staining (In Situ Cell Death Detection Kit, Roche) was performed following the manufacturer's instruction. The sections were visualized under a fluorescence microscope Leica DMi8.

Quantification and Statistical Analysis

Microthrombi counts were performed as previously described [23]. Predefined regions of interest (ROIs) were photographed at ×200 magnification. The cumulative number of microthrombi was counted in a blinded fashion. The data were expressed as means ± SD. One-way analysis of variance (ANOVA) was used in this study to compare means of different groups followed by a Tukey's multiple comparison test. The statistical analysis was carried out using SPSS 16.0 software (SPSS Inc., Chicago, Illinois, USA). Statistically significance was accepted with $p < 0.05$.

Results

General Observation and SAH Severity and Localization of SAH

A total of 107 rats were used. Eighteen rats were sham group and 87 rats underwent SAH. Two rats were excluded from the study due to mild SAH. At 24 h after SAH induction, blood clots were mainly observed around the Willis circle and ventral brainstem (Fig. 1a). No statistical differences in the average of SAH grades were observed between SAH groups (Fig. 1b). About 17.2% rats (15 of 87) under SAH condition died within 24 h after SAH induction. No animals died in the sham group (0 of 18 rats). No statistical significance was observed for mortality between operated groups.

Time Course of HSP90 Detected in the Left Hemisphere and Microthrombosis in the Cerebellum Following SAH

Western blot was performed to determine the HSP90 expression in the left hemisphere at the 1, 2, 3, and 5 days after SAH. Results showed that HSP90 level increased as early as 1 day after SAH and peaked 2 days and then decreased (Fig. 2a). Quantitative analyses of HSP90 time course show nearly 2.8 times higher at 2 days when compared with sham group (Fig. 2a). Immunohistochemistry was performed to detect the microthrombosis at same time point (Fig. 2b). Results showed that microthrombi counts increased as early as 1 day after SAH and peaked 2 days and then decreased (Fig. 2c).

HSP90 Inhibitor 17-AAG Treatment Reduces RIP3 and NLRP3 Inflammasome, Ameliorates Microthrombosis, and Improves Short-Term Neurobehavior

The modified Garcia and beam balance scores were significantly lower in the SAH + vehicle group than those in the sham group, and administration of 17-AAG improved the neurological scores in SAH + 17-AAG group significantly compared with SAH + vehicle group ($P < 0.05$; Fig. 1c, d). At 2 days after SAH, the expression of HSP90 was remarkably increased, and RIP3, NLRP3, ASC, and IL-1β were dramatically increased in SAH + vehicle group compared with the sham group. However, 17-AAG treatment reduced the level of HSP90 and inhibited the expression of RIP3, NLRP3,

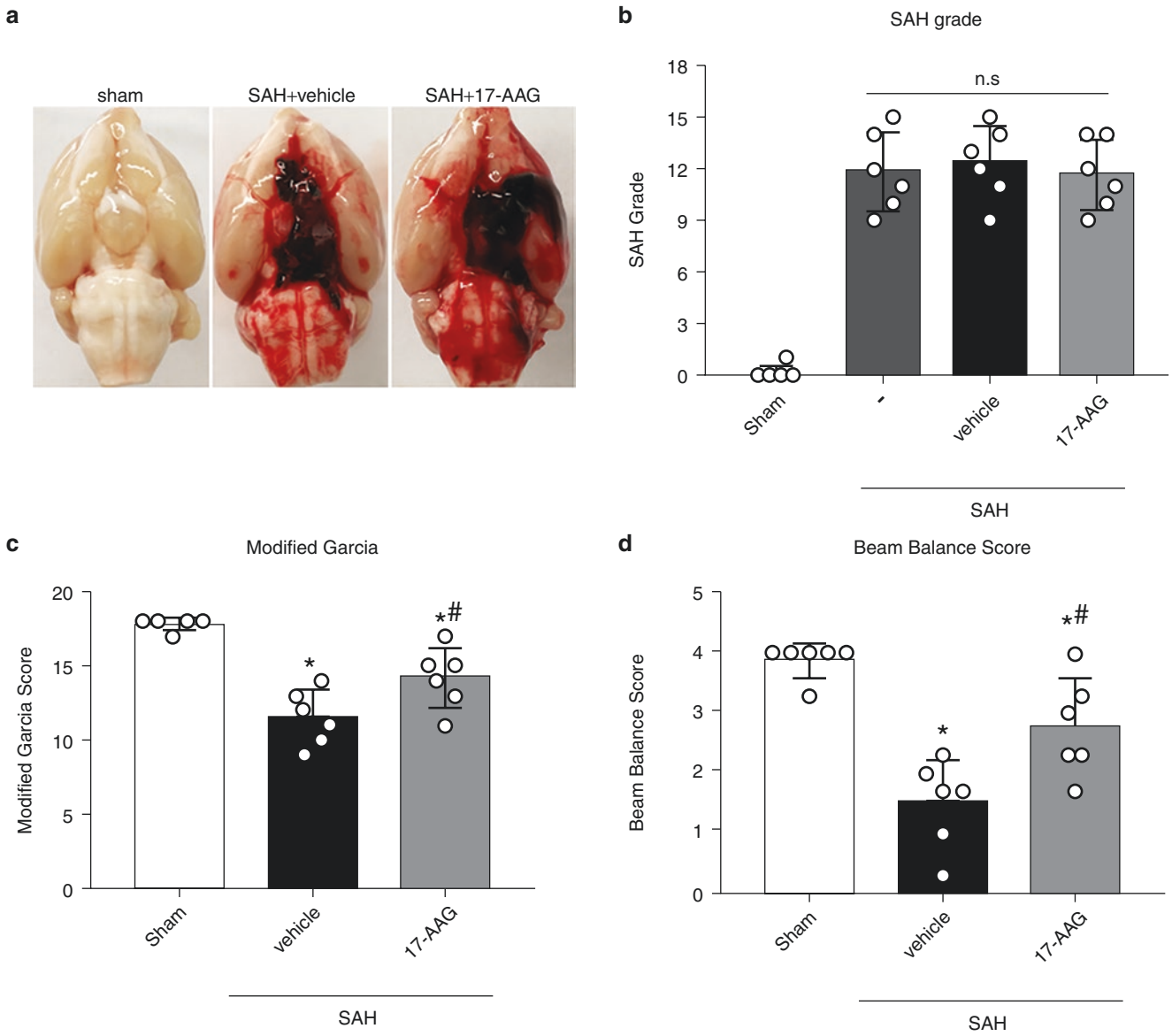

Fig. 1 General observation and SAH grade and neurological score. (**a**) Representative images of the brains from each group at 24 h after operation. Subarachnoid blood clots were mainly around the Willis circle and ventral brainstem. No blood present in the sham group. (**b**) There were no significant difference of SAH grade between the SAH groups ($p < 0.05$). Similar SAH bleeding severity was observed in all SAH groups. (**c**) Modified Garcia score and (**d**) beam balance test between sham, SAH + vehicle, and SAH + 17-AAG group. $n = 6$ per group. $^{*}p < 0.05$ vs. sham, $\#p < 0.05$ vs. SAH + vehicle

ASC, and IL-1β in SAH + 17-AAG group when compared with SAH + vehicle group ($P < 0.05$; Fig. 3a). When co-labeling with TUNEL and vessel marker lectin, the results show the endothelial cells on the inner surface vessels under apoptosis in SAH + vehicle when compared to sham; however the 17-AAG treatment can reverse this change (Fig. 3b, c). The microthrombosis was remarkably increased at 2 days in SAH + vehicle group compared with the sham group. However, 17-AAG treatment reduced microthrombosis when compared with SAH + vehicle group ($P < 0.05$; Fig. 3d, e).

Discussion

In the present study, we found that both microthrombosis and the expression of HSP90 increased in the brain after SAH in rats. In addition, the 17-AAG treatment improved neurofunction after SAH, which were accompanied by a decrease in RIP3 and NLRP3 inflammasome expression. Furthermore, 17-AAG showed the neuroprotective effects after SAH, which were associated with the decreased microthrombosis 2 days after SAH.

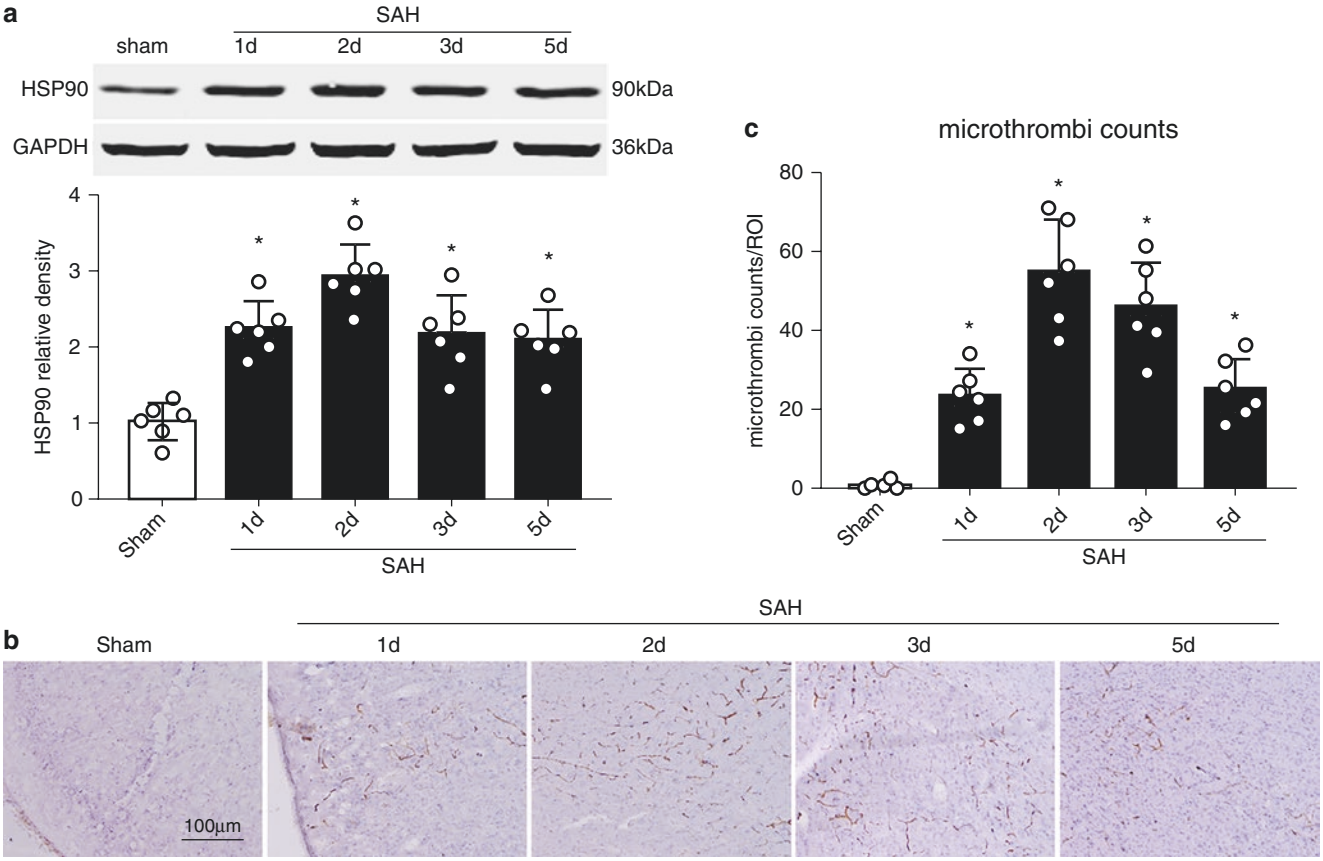

Fig. 2 Microthrombosis in cerebellum and expression HSP90 in left hemisphere after SAH. (**a**) Representative Western blot images and quantitative analyses of HSP90 time course from the left hemisphere after SAH. (**b**) Representative image and (**c**) quantitative analyses of microthrombosis in sham and SAH group with different time point. $n = 6$ per group. $^*p < 0.05$ vs. sham

The role of NLRP3 inflammasome in the pathophysiology of EBI after SAH has been proved previously [12]. The NLRP3 form a complex with ASC and pro-caspase-1 when activated and then maturate IL-1β and IL-18 by cleaved caspase-1 contributes to inflammation after SAH [12]. ROS generation, K+ efflux, and Cl− efflux were proved be three common upstream of NLRP3 activation [25]. Recently, RIP3 has been elucidated to have regulated NLRP3 inflammasome after SAH [4]. HSP90, as a chaperone protein, has been proven to show its effect on ischemia stroke. HSP90 inhibitors such as 17-AAG show its protective effects in ischemia stroke by attenuating inflammatory responses, ameliorating neuronal autophagic death, and protecting neural progenitor cell death and blood-brain barrier from disruption [16, 17, 26, 27]. More recently, HSP90 as a direct upstream regulator of RIP3 has been proved in neuronal oxygen-glucose deprivation model, and inhibition of HSP90 protected neurons from necroptosis [20]. Interestingly, a clinical study show that the antibody level of heat shock proteins increased in stroke patients [28]. However, the HSP90 regulate the NLRP3 activation after SAH have not been elucidated. In our present study, we found that HSP90 increased 1 day and peaked 2 days after SAH, and administration of HSP90 inhibitor 17-AAG reduced inflammation via HSP90/RIP3/NLRP3 signaling pathway as well as improve neurofunction.

Microthrombosis, as well as pro-inflammatory cascades and blood-brain barrier disruption, consist the main cascade events of secondary injury after SAH. One of the main causes of microthrombi formation after SAH was endothelial cell injury [10]. What's more, endothelial apoptosis after SAH has been shown to be associated with inflammatory mediators such as interleukin-1β (IL-1β) [7, 29]. In the present study, our results show that 17-AAG can reduce IL-1β by inhibiting NLRP3 inflammasome formation and then reduce microthrombosis after SAH. Thus, reduce NLRP3 inflammasome mediated inflammatory response by administration of 17-AAG may be a pential target to therapy microthrombosis after SAH.

These findings suggested that the administration of 17-AAG could attenuate NLRP3 inflammasome activation, inhibit microthrombosis, and improve neurofunction after SAH, at least, in part, through the HSP90/RIP3/NLRP3 signaling pathway.

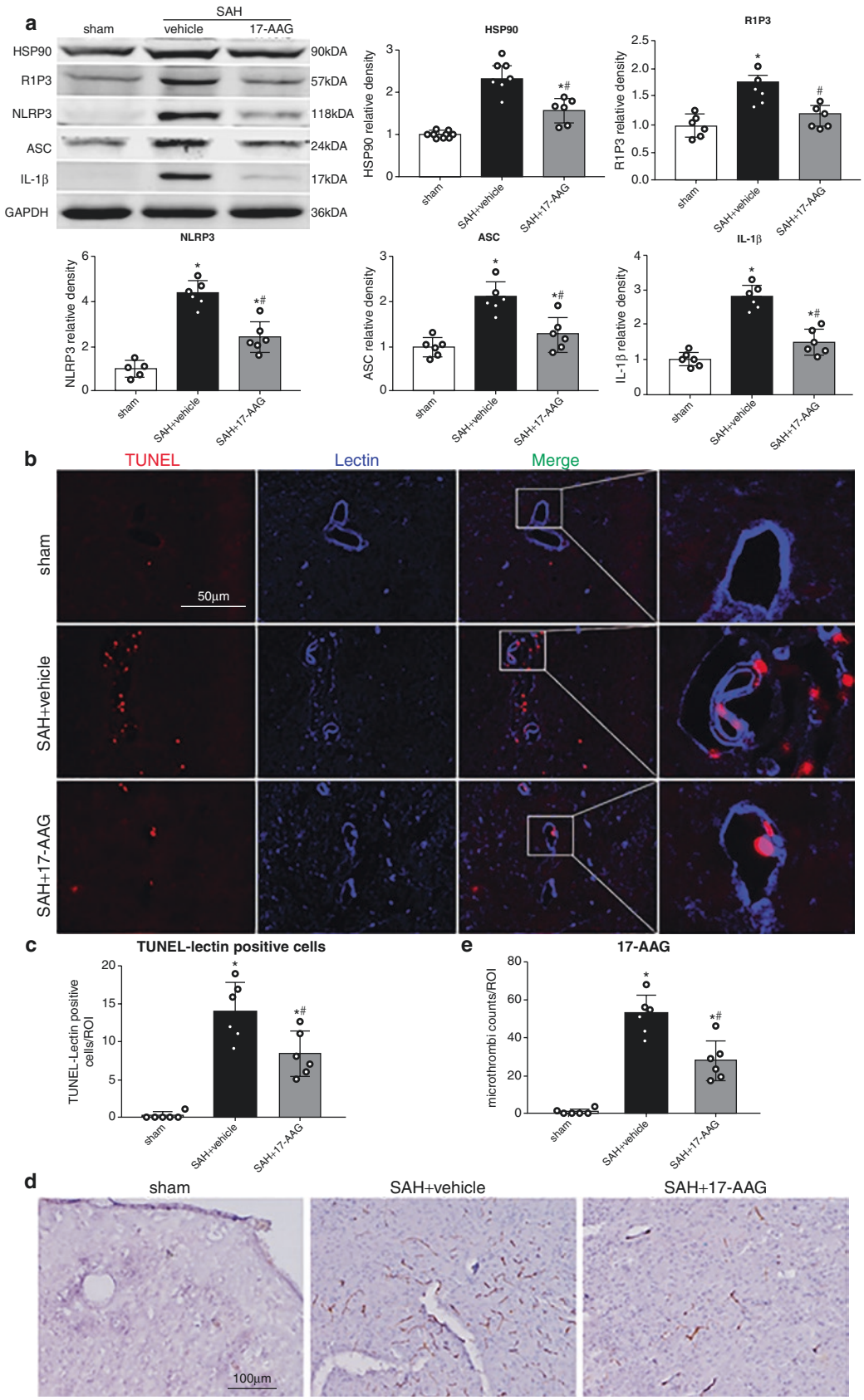

Fig. 3 The effects of 17-AAG in the protein expression of RIP3, NLRP3, ASC, IL-1β, and microthrombosis. (**a**) Representative Western blot images and quantitative analyses of HSP90, RIP3, NLRP3, ASC, and IL-1β. $n = 6$ per group. *$P < 0.05$ vs. sham group; #$P < 0.05$, vs. SAH + vehicle group. Bars represent mean ± SD. (**b**) Representative image and (**c**) quantitative analyses of double staining of TUNEL and lectin. (**d**) Immunostaining of fibrinogen and (**e**) quantitative analyses of microthrombi. $n = 6$ per group. *$P < 0.05$ vs. sham group; #$P < 0.05$, vs. SAH + vehicle group

Conclusion

Our study showed that 17-AAG can improve neurofunction and alleviate inflammation through the HSP90/RIP3/NLRP3 pathway as well as reduce microthrombosis after SAH. It may provide an optical method to treatment of SAH.

Acknowledgments This project was funded by Grant 81571150 from National Natural Science Foundation of China.

Conflict of Interest: **The authors declare that they have no conflict of interest.**

References

1. Lapchak PA, Zhang JH. The high cost of stroke and stroke cytoprotection research. Transl Stroke Res. 2017;8:307–17.
2. Caner B, Hou J, Altay O, Fujii M, Zhang JH. Transition of research focus from vasospasm to early brain injury after subarachnoid hemorrhage. J Neurochem. 2012;123(Suppl 2):12–21.
3. Fujii M, Yan J, Rolland WB, Soejima Y, Caner B, Zhang JH. Early brain injury, an evolving frontier in subarachnoid hemorrhage research. Transl Stroke Res. 2013;4:432–46.
4. Zhou K, Shi L, Wang Z, Zhou J, Manaenko A, Reis C, Chen S, Zhang J. RIP1-RIP3-DRP1 pathway regulates NLRP3 inflammasome activation following subarachnoid hemorrhage. Exp Neurol. 2017;295:116–24.
5. Khalafalla MG, Woods LT, Camden JM, Khan AA, Limesand KH, Petris MJ, Erb L, Weisman GA. P2X7 receptor antagonism prevents IL-1beta release from salivary epithelial cells and reduces inflammation in a mouse model of autoimmune exocrinopathy. J Biol Chem. 2017;292:16626–37.
6. Chen S, Ma Q, Krafft PR, Hu Q, Rolland W II, Sherchan P, Zhang J, Tang J, Zhang JH. P2X7R/cryopyrin inflammasome axis inhibition reduces neuroinflammation after SAH. Neurobiol Dis. 2013;58:296–307.
7. Vergouwen MD, Vermeulen M, Coert BA, Stroes ES, Roos YB. Microthrombosis after aneurysmal subarachnoid hemorrhage: an additional explanation for delayed cerebral ischemia. J Cereb Blood Flow Metab. 2008;28:1761–70.
8. Suzuki S, Kimura M, Souma M, Ohkima H, Shimizu T, Iwabuchi T. Cerebral microthrombosis in symptomatic cerebral vasospasm--a quantitative histological study in autopsy cases. Neurol Med Chir (Tokyo). 1990;30:309–16.
9. Andereggen L, Neuschmelting V, von Gunten M, Widmer HR, Fandino J, Marbacher S. The role of microclot formation in an acute subarachnoid hemorrhage model in the rabbit. Biomed Res Int. 2014;2014:161702.
10. Sabri M, Ai J, Lakovic K, D'Abbondanza J, Ilodigwe D, Macdonald RL. Mechanisms of microthrombi formation after experimental subarachnoid hemorrhage. Neuroscience. 2012;224:26–37.
11. Pisapia JM, Xu X, Kelly J, Yeung J, Carrion G, Tong H, Meghan S, El-Falaky OM, Grady MS, Smith DH, Zaitsev S, Muzykantov VR, Stiefel MF, Stein SC. Microthrombosis after experimental subarachnoid hemorrhage: time course and effect of red blood cell-bound thrombin-activated pro-urokinase and clazosentan. Exp Neurol. 2012;233:357–63.
12. Dong YS, Fan CX, Hu W, Jiang S, Ma ZQ, Yan XL, Deng C, Di SY, Xin ZL, Wu GL, Yang Y, Reiter RJ, Liang GB. Melatonin attenuated early brain injury induced by subarachnoid hemorrhage via regulating NLRP3 inflammasome and apoptosis signaling. J Pineal Res. 2016;60:253–62.
13. Li D, Li C, Li L, Chen S, Wang L, Li Q, Wang X, Lei X, Shen Z. Natural product Kongensin A is a non-canonical HSP90 inhibitor that blocks RIP3-dependent necroptosis. Cell Chem Biol. 2016;23:257–66.
14. Zhao XM, Chen Z, Zhao JB, Zhang PP, Pu YF, Jiang SH, Hou JJ, Cui YM, Jia XL, Zhang SQ. Hsp90 modulates the stability of MLKL and is required for TNF-induced necroptosis. Cell Death Dis. 2016;7:e2089.
15. Pasparakis M, Vandenabeele P. Necroptosis and its role in inflammation. Nature. 2015;517:311–20.
16. Qi J, Han X, Liu HT, Chen T, Zhang JL, Yang P, Bo SH, Lu XT, Zhang J. 17-Dimethylaminoethylamino-17-demethoxygeldanamycin attenuates inflammatory responses in experimental stroke. Biol Pharm Bull. 2014;37:1713–8.
17. Qi J, Liu Y, Yang P, Chen T, Liu XZ, Yin Y, Zhang J, Wang F. Heat shock protein 90 inhibition by 17-Dimethylaminoethylamino-17-demethoxygeldanamycin protects blood-brain barrier integrity in cerebral ischemic stroke. Am J Transl Res. 2015;7:1826–37.
18. Wang X, Jiang W, Yan Y, Gong T, Han J, Tian Z, Zhou R. RNA viruses promote activation of the NLRP3 inflammasome through a RIP1-RIP3-DRP1 signaling pathway. Nat Immunol. 2014;15:1126–33.
19. Park SY, Shim JH, Chae JI, Cho YS. Heat shock protein 90 inhibitor regulates necroptotic cell death via down-regulation of receptor interacting proteins. Pharmazie. 2015;70:193–8.
20. Wang Z, Guo LM, Wang Y, Zhou HK, Wang SC, Chen D, Huang JF, Xiong K. Inhibition of HSP90alpha protects cultured neurons from oxygen-glucose deprivation induced necroptosis by decreasing RIP3 expression. J Cell Physiol. 2018;233:4864–84.
21. Liao F, Li G, Yuan W, Chen Y, Zuo Y, Rashid K, Zhang JH, Feng H, Liu F. LSKL peptide alleviates subarachnoid fibrosis and hydrocephalus by inhibiting TSP1-mediated TGF-β1 signaling activity following subarachnoid hemorrhage in rats. Exp Ther Med. 2018;12:2537–43.
22. Liu F, Chen Y, Hu Q, Li B, Tang J, He Y, Guo Z, Feng H, Tang J, Zhang JH. MFGE8/integrin beta3 pathway alleviates apoptosis and inflammation in early brain injury after subarachnoid hemorrhage in rats. Exp Neurol. 2015;272:120–7.
23. Muroi C, Fujioka M, Mishima K, Irie K, Fujimura Y, Nakano T, Fandino J, Keller E, Iwasaki K, Fujiwara M. Effect of ADAMTS-13 on cerebrovascular microthrombosis and neuronal injury after experimental subarachnoid hemorrhage. J Thromb Haemost. 2014;12:505–14.
24. Xiao Y, Li G, Chen Y, Zuo Y, Rashid K, He T, Feng H, Zhang JH, Liu F. Milk fat globule-epidermal growth factor-8 pretreatment attenuates apoptosis and inflammation via the integrin-β3 pathway after surgical brain injury in rats. Front Neurol. 2018;9:96.
25. Tang T, Lang X, Xu C, Wang X, Gong T, Yang Y, Cui J, Bai L, Wang J, Jiang W, Zhou R. CLICs-dependent chloride efflux is an essential and proximal upstream event for NLRP3 inflammasome activation. Nat Commun. 2017;8:202.
26. Li J, Yang F, Guo J, Zhang R, Xing X, Qin X. 17-AAG post-treatment ameliorates memory impairment and hippocampal CA1 neuronal autophagic death induced by transient global cerebral ischemia. Brain Res. 2015;1610:80–8.
27. Bradley E, Zhao X, Wang R, Brann D, Bieberich E, Wang G. Low dose Hsp90 inhibitor 17AAG protects neural progenitor cells from ischemia induced death. J Cell Commun Signal. 2014;8:353–62.
28. Banecka-Majkutewicz Z, Grabowski M, Kadzinski L, Papkov A, Wegrzyn A, Banecki B. Increased levels of antibodies against heat shock proteins in stroke patients. Acta Biochim Pol. 2014;61:379–83.
29. Zhou C, Yamaguchi M, Kusaka G, Schonholz C, Nanda A, Zhang JH. Caspase inhibitors prevent endothelial apoptosis and cerebral vasospasm in dog model of experimental subarachnoid hemorrhage. J Cereb Blood Flow Metab. 2004;24:419–31.